Effects of substrate-induced strain on transport properties of LaMnO$_{3+\delta}$ and CaMnO$_3$ thin films using ferroelectric poling and converse piezoelectric effect

R. K. Zheng,[1,2] H.-U. Habermeier,[1] H. L. W. Chan,[2] C. L. Choy,[2] and H. S. Luo[3]

[1]*Max Planck Institute for Solid State Research, Heisenbergstrasse 1, D-70569 Stuttgart, Germany*
[2]*Department of Applied Physics and Materials Research Center, The Hong Kong Polytechnic University, Hong Kong, China*
[3]*State Key Laboratory of High Performance Ceramics and Superfine Microstructure, Shanghai Institute of Ceramics, Chinese Academy of Sciences, Shanghai 201800, China*

We have investigated the effects of the strain induced by ferroelectric poling (or the converse piezoelectric effect) on the transport properties of LaMnO$_{3+\delta}$ and CaMnO$_3$ thin films grown on ferroelectric 0.67Pb(Mg$_{1/3}$Nb$_{2/3}$)O$_3$-0.33PbTiO$_3$ single-crystal substrates. The ferroelectric poling of the substrate gives rise to a reduction in the in-plane tensile strain of the LaMnO$_{3+\delta}$ film, which results in a significant decrease in the resistance and increase in the insulator-to-metal transition temperature T_P of the film. The ferroelectric poling also leads to opposite effects on the magnetoresistance (MR) below and above T_P, namely, MR is reduced for $T < T_P$ while MR is enhanced for $T > T_P$. These strain effects are explained in terms of coexisting phases whose volume fractions are modified as a result of the reduction in the Jahn-Teller (JT) distortion due to ferroelectric poling. An investigation of the effects of the strain induced by the converse piezoelectric effect on the resistance of the LaMnO$_{3+\delta}$ and CaMnO$_3$ films shows that the resistance-strain coefficients $(\Delta R/R)/(\Delta c_{film}/c_{film})$ of the LaMnO$_{3+\delta}$ film is much larger than those of the CaMnO$_3$ film. This result may imply that the strain-induced modification of the electronic bandwidth alone cannot account for the large $(\Delta R/R)/(\Delta c_{film}/c_{film})$ observed in the LaMnO$_{3+\delta}$ film, and highlights that the strong coupling of charge carriers to JT distortion is crucial for understanding the effects of the substrate-induced strain in manganite thin films.

I. INTRODUCTION

Lanthanum-based mixed-valent manganites La$_{1-x}$A$_x$MnO$_3$ (A=Ca, Sr, and Ba) have attracted considerable attention in the last decade due to their interesting physical properties and potential device applications.[1] The parent compound, LaMnO$_3$, is an insulating material which shows simultaneous cooperative Jahn-Teller (JT) distortion of MnO$_6$ octahedra and $d_{3x^2-r^2}/d_{3y^2-r^2}$ orbital order below T_{JT}=750 K.[2] Quite a number of experimental studies have shown that LaMnO$_3$ compounds exhibit a wide range of oxygen nonstoichiometry,[3–8] as reflected in the general formula LaMnO$_{3+\delta}$. The excess of oxygen causes the valence state of a portion of the manganese ions to change from Mn^{3+} to Mn^{4+} and thus suppresses the cooperative JT distortion and $d_{3x^2-r^2}/d_{3y^2-r^2}$ orbital ordering, which consequently results in substantial changes in the structural, magnetic, and transport properties of LaMnO$_{3+\delta}$ compounds.[3–7]

As δ increases, the crystallographic structure evolves from the highly JT distorted orthorhombic structure (*Pbmn*, $c/\sqrt{2}<a<b$) for $0 \le \delta \le 0.04$ to the slightly JT-distorted orthorhombic structure (*Pbmn*, $a \le c/\sqrt{2}<b$), and subsequently, to the rhombohedral structure for $\delta > 0.1$.[3,4] At the same time, the magnetic ground state evolves from the canted antiferromagnetic (AFM) for $\delta < 0.05$ to mixed AFM ferromagnetic (FM) for $0.05 \le \delta \le 0.11$, and then to FM for $0.11 < \delta \le 0.14$, and finally to metamagnetic canted-spin configuration for $0.14 < \delta \le 0.18$.[5] For the transport properties, controversial results have been reported for close δ, Ritter *et al.*[3] and Louca *et al.*[6] reported that the δ=0.1 compound has a rhombohedral crystallographic symmetry and

$T_C \sim 150$–155 K while Choi *et al.*[7] reported that the δ =0.096 compound has a orthorhombic crystallographic symmetry and $T_C \sim 186$ K. All these results demonstrate that the properties of nonstoichiometric LaMnO$_{3+\delta}$ compounds are very sensitive to the excess of oxygen. Therefore, when one studies the strain effects of LaMnO$_{3+\delta}$ thin films, it is very important that the investigated LaMnO$_{3+\delta}$ films have the same δ since the properties of LaMnO$_{3+\delta}$ is so sensitive to δ.

Ritter *et al.*[3] performed measurements of ac initial magnetic susceptibility, magnetization, magnetoresistance (MR), and neutron-diffraction measurements on a series of LaMnO$_{3+\delta}$ samples and found that, as δ increases from 0 to 0.07, a small fraction of FM metallic phase appears due to the local Mn^{3+}-O-Mn^{4+} double exchange interaction. The local FM metallic phase coexists with the AFM insulating phase. They further found that for δ=0.07 and 0.1 samples, charge-ordered (CO) phase emerges at low temperatures below ~ 110 K, well below the ferromagnetic ordering temperature (~ 150 K), pointing to the coexistence of CO phase and FM metallic phase at low temperatures. Since the JT distortion plays a very important role in localizing the e_g electrons, it is expected that a change in the magnitude of the JT distortion would lead to significant changes in the volume fraction of the coexistence phases and hence the transport and magnetic properties of the LaMnO$_{3+\delta}$ compounds.

Although the properties of LaMnO$_{3+\delta}$ compounds in bulk form have been studied extensively, investigations on the properties of nonstoichiometric LaMnO$_{3+\delta}$ thin films are very limited. Particularly, the effects of substrate-induced strain on the JT distortion and phase separation in LaMnO$_{3+\delta}$ thin films are still unknown. In this work, we deposited

LaMnO$_{3+\delta}$ films (for which the JT distortion is significant) and CaMnO$_3$ films (for which there is no JT distortion) on ferroelectric 0.67Pb(Mg$_{1/3}$Nb$_{2/3}$)O$_3$-0.33PbTiO$_3$ (PMN-PT) single-crystal substrates whose in-plane strain can be dynamically changed via ferroelectric poling or the converse piezoelectric effect[9–15] and studied the effects of the strain induced by ferroelectric poling or the converse piezoelectric effect on the JT distortion, phase separation, and transport properties of the films. Since we dynamically change the strain state of the films using the same LaMnO$_{3+\delta}$/PMN-PT or CaMnO$_3$/PMN-PT sample, therefore the effects of oxygen nonstoichiometry δ on the properties of the films are kept constant.

We have observed that the induced strain in the PMN-PT substrate was effectively transferred to the film, causing a reduction in the in-plane tensile strain of the LaMnO$_{3+\delta}$ film. Consequently, the JT distortion, phase separation, and transport properties of the LaMnO$_{3+\delta}$ film are modified. Moreover, we give experimental evidence that the electron-lattice coupling due to the JT distortion plays a crucial role in determining the substrate-induced strain effects in LaMnO$_{3+\delta}$ films by comparing the resistance-strain coefficients $(\Delta R/R)/(\Delta c_{film}/c_{film})$ of LaMnO$_{3+\delta}$ films with those of CaMnO$_3$ films.

II. EXPERIMENTAL DETAILS

PMN-PT single crystals with dimensions of $\Phi 48 \times 80$ mm^2 were grown by a modified Bridgman technique[16] at the Shanghai Institute of Ceramics. The crystals were cut into rectangular plates ($10 \times 2.5 \times 0.5$ mm^3) with the plate normal in the $\langle 001 \rangle$ crystal direction and polished to a surface roughness of less than 1 nm. LaMnO$_{3+\delta}$ and CaMnO$_3$ films were deposited on the (001)-oriented and polished PMN-PT substrates using dc magnetron sputtering. The deposition was carried out in an argon-oxygen flow with 60% Ar and 40% O$_2$ at a pressure of 5 Pa and a substrate temperature of 700 °C. During deposition, the substrate holder rotates slowly in order to reduce the dispersion of film thickness over the whole film. After deposition, the films were *in situ* cooled to room temperature and postannealed in air at 700 °C for 30 min using a rapid thermal processor furnace.

X-ray diffraction (XRD) patterns of the LaMnO$_{3+\delta}$/PMN-PT and CaMnO$_3$/PMN-PT structures were recorded using a four-circle Bruker D8 Discover x-ray diffractometer equipped with Cu $K\alpha_1$ radiation. For *in situ* XRD measurements, the electric potentials applied to the LaMnO$_{3+\delta}$/PMN-PT (or the CaMnO$_3$/PMN-PT) structure was changed from 0 to 10 kV/cm in steps of 0.5 or 1 kV/cm while all other parameters were kept constant after the alignment of the x-ray beam. The measurements were made in the 2θ range from 44° to 50° at 295 K during the application of an electric field E ($0 \leq E \leq 10$ kV/cm) to the LaMnO$_{3+\delta}$/PMN-PT (or the CaMnO$_3$/PMN-PT) structure. A schematic of the electric field configuration for *in situ* XRD measurements is shown in the inset (a) of Fig. 1. XRD θ-2θ scan of the LaMnO$_{3+\delta}$/PMN-PT structure indicates that the LaMnO$_{3+\delta}$ film is c-axis preferentially oriented and has no
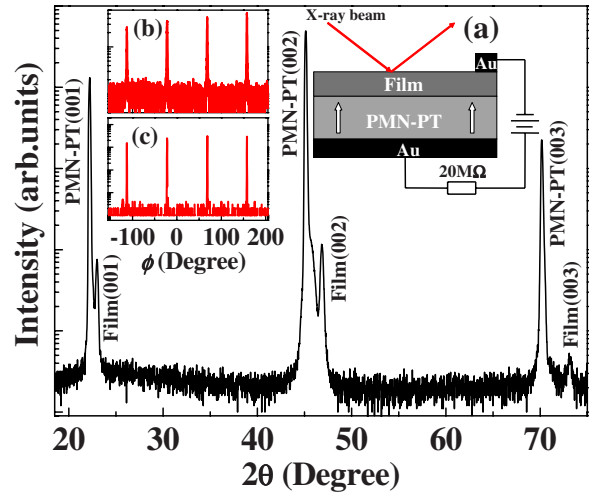

FIG. 1. (Color online) X-ray diffraction pattern of the LaMnO$_{3+\delta}$/PMN-PT structure. Inset (a) shows a schematic of the electric field configuration for *in situ* XRD measurements. The arrow in the inset (a) represents the poling direction. Insets (b) and (c) show the XRD ϕ scans on the LaMnO$_{3+\delta}$(101) and PMN-PT(101) reflections, respectively.

secondary phases (see Fig. 1). We also performed XRD ϕ scans on the LaMnO$_{3+\delta}$(101) and PMN-PT(101) reflections, respectively, and observed a fourfold symmetrical reflection for both the LaMnO$_{3+\delta}$ film and the PMN-PT substrate [insets (b) and (c) of Fig. 1, respectively], indicating the epitaxial growth of the LaMnO$_{3+\delta}$ film on the PMN-PT substrate. Since the dispersion of oxygen content may result in structural inhomogeneity,[8] we thus made XRD measurements on the LaMnO$_{3+\delta}$/PMN-PT structure when the incident x-ray beam is in the longitudinal and transversal configurations with respect to the film square, respectively. We found that the 2θ values of the PMN-PT(002) and LaMnO$_{3+\delta}$(002) reflections for longitudinal configuration are the same as those for transversal configuration, which implies that the dispersion of oxygen content and film thickness over the whole film is small and can be neglected.

The inset (a) of Fig. 2 shows the circuit for electrical resistance measurements. A physical property measurement system (PPMS 9T, Quantum Design) was used to measure the resistance of the LaMnO$_{3+\delta}$ film between the two top-top gold electrodes in the temperature range 10–300 K and in a magnetic field (up to 9 T) applied parallel to the film plane. The resistance of the PMN-PT substrate was estimated to be $\sim 3 \times 10^9$ Ω at room temperature by measuring the leakage current in the PMN-PT substrate using a Keithley 6517A electrometer. Since the resistance ($\sim 1.3 \times 10^4$ Ω at room temperature) of the conducting LaMnO$_{3+\delta}$ (or CaMnO$_3$) film is much smaller than that of the PMN-PT substrate, the LaMnO$_{3+\delta}$ (or the CaMnO$_3$) film, in fact, serves as the top electrode for poling the PMN-PT substrate. This was achieved by applying a dc poling field E (E is much larger than the coercive field E_C of the PMN-PT substrate) to the LaMnO$_{3+\delta}$/PMN-PT (or the CaMnO$_3$/PMN-PT) structure through the film (top electrode) and bottom gold electrodes using a Model PS325 high-voltage power supply (Stanford Research Systems, Inc.). Note that the top electrode was al-
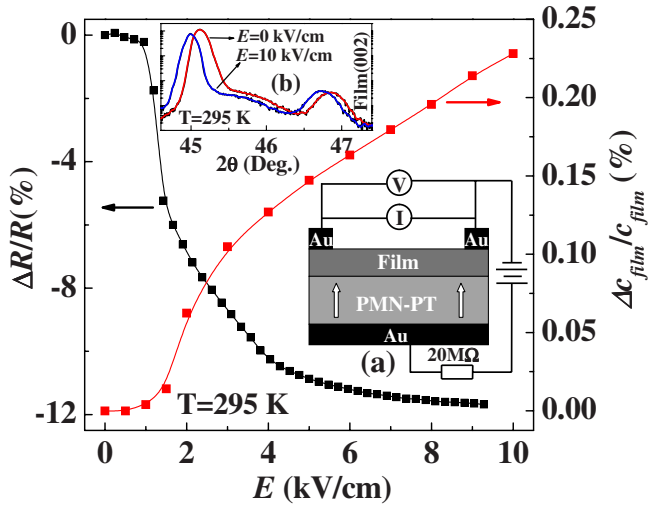
FIG. 2. (Color online) Relative change in the lattice constant c and resistance of the LaMnO$_{3+\delta}$ film as a function of the electric field applied to the LaMnO$_{3+\delta}$/PMN-PT structure through the top and bottom electrodes. Inset (a) shows the circuit for electrical resistance measurements. Inset (b) shows the XRD patterns in the vicinity of (002) reflections for the LaMnO$_{3+\delta}$/PMN-PT structure under zero electric field and an electric field of 10 kV/cm. The initial poling state of the PMN-PT substrate is in P_r^0.

ways held at zero electric potential. The magnetic properties of the LaMnO$_{3+\delta}$ films were measured using a superconducting quantum interference device (SQUID-VSM 7T, Quantum Design) magnetometer with the magnetic field applied parallel to the film plane.

III. RESULTS AND DISCUSSION

A. LaMnO$_{3+\delta}$/PMN-PT structure

1. Effects of ferroelectric poling on the resistance and strain of the film

First, we studied the effects of the strain induced by ferroelectric poling on the transport properties of the LaMnO$_{3+\delta}$ film at a fixed temperature of 295 K. The resistance of the LaMnO$_{3+\delta}$ film between the two top-top gold electrodes was measured as a function of the electric field E applied to the LaMnO$_{3+\delta}$/PMN-PT structure through the top and bottom electrodes. It should be pointed out that initially the PMN-PT substrate was in unpoled state (denoted by P_r^0) and the electric field was increased from 0 to ~9.3 kV/cm in steps of ~0.24 kV/cm. The electric field induced relative change in the resistance, $\Delta R/R$, is plotted as a function of E in Fig. 2. Here, $\Delta R/R$ is defined as $\Delta R/R = [R(E) - R(0)]/R(0)$, where $R(E)$ and $R(0)$ are the resistances of the LaMnO$_{3+\delta}$ film under an electric field E and zero electric field, respectively. The resistance is almost field independent for $E \leq 1$ kV/cm, but decreases drastically with further increase in E. For $E > 4$ kV/cm, the resistance decreases gently with increasing E, implying that the poling of the PMN-PT substrate is almost completed below 4 kV/cm. We note that a similar electric field induced decrease in the resistance has been observed in La$_{1-x}$Ba$_x$MnO$_3$ $(x=0.125, 0.3)$/PMN-PT

structure,[13,14] which was found to be due to a change in the strain state of the film induced by ferroelectric poling of the PMN-PT substrate.

We performed *in situ* XRD measurements on a LaMnO$_{3+\delta}$/PMN-PT structure. Selected XRD patterns in the vicinity of the (002) reflection under $E=0$ and 10 kV/cm are shown in the inset (b) of Fig. 2. The results indicate that both the PMN-PT(002) and LaMnO$_{3+\delta}$(002) reflections shift toward lower 2θ values when an electric field E $(E > E_C)$ is applied to the LaMnO$_{3+\delta}$/PMN-PT structure. When the PMN-PT substrate is in P_r^0 state, i.e., $E=0$ kV/cm, the lattice constant c of the LaMnO$_{3+\delta}$ film is calculated to be ~3.875 Å. We recall that the lattice constants of the LaMnO$_{3+\delta}$ bulk materials vary with δ.[3–7] By comparing the onset temperature of ferromagnetic ordering and the charge-ordering transition temperature T_{CO} of the LaMnO$_{3+\delta}$ film (which will be discussed in the following section) with those of LaMnO$_{3+\delta}$ bulk materials,[4,7] it is roughly estimated that the LaMnO$_{3+\delta}$ film has an excess oxygen $\delta \sim 0.09$. For δ ~ 0.09, the lattice constant c of the LaMnO$_{3+\delta}$ single crystal is ~3.903 Å.[4,7] This value is larger than that of the LaMnO$_{3+\delta}$ film, indicating that the film is subjected to an out-of-plane compressive and an in-plane tensile strain, in agreement with the fact that the lattice constants of the LaMnO$_{3+\delta}$ bulk materials are smaller than those $[a \sim b \sim c \sim 4.02$ Å (Ref. 17)] of the PMN-PT substrate.

As can be seen in Fig. 2, the electric field induces a significant increase in the lattice constant c of the LaMnO$_{3+\delta}$ film. c is slightly dependent on E for $E \leq 1$ kV/cm, but increases remarkably with increasing E from 1.5 kV/cm. For $E > 4$ kV/cm, c increases almost linearly. We note that, when an electric field of 10 kV/cm is applied to the LaMnO$_{3+\delta}$/PMN-PT structure, the lattice constant c (~3.884 Å) of the film is still smaller than that of the LaMnO$_{3+\delta}$ $(\delta=0.09)$ bulk material, indicating that the film is still under in-plane tensile strain, although the in-plane tensile strain has been considerably reduced. For an unpoled ferroelectric material, the application of an electric field to the material would induce a nonlinear increase in the lattice constants near E_C of the ferroelectric material due to the rotation of the polarization of the ferroelectric domains toward the field direction.[18] The observed nonlinear increase in the lattice constant c of the LaMnO$_{3+\delta}$ film near E $=2$ kV/cm (which is close to E_C of the PMN-PT substrate[14]) is undoubtedly due to the ferroelectric-poling-induced in-plane compressive strain in the PMN-PT substrate. This induced strain was transferred to the film and thus cause a reduction in the in-plane tensile of the film, which reduces the JT distortion of MnO$_6$ (Ref. 19) and thus a weakening of the electron-lattice coupling, favoring the itinerancy of charge carriers.[20]

We point out that the ferroelectric field effect in the LaMnO$_{3+\delta}$/PMN-PT structure is negligible. If the ferroelectric field effect plays a dominant role in influencing the transport properties of the LaMnO$_{3+\delta}$ film, the resistance electric field (R-E) hysteresis loop should show a squarelike shape with the resistance change exhibiting opposite signs for opposite directions of applied electric field, as previously observed in La$_{1-x}$Ba$_x$MnO$_3$ $(x=0.1, 0.15)$/Pb(Zr$_{0.2}$Ti$_{0.8}$)TiO$_3$ (Ref. 21) and La$_{0.8}$Ca$_{0.2}$MnO$_3$/Pb(Zr$_{0.2}$Ti$_{0.8}$)TiO$_3$ (Ref. 22)
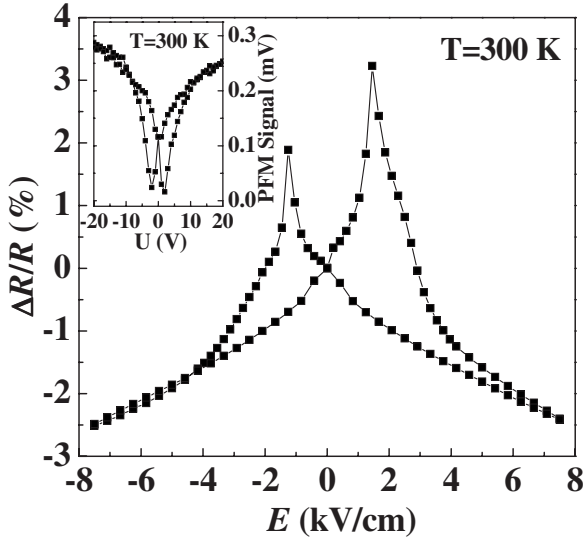
FIG. 3. Relative change in the resistance of the LaMnO$_{3+\delta}$ film between the two top-top gold electrodes at 300 K as a function of bipolar electric field applied to the PMN-PT substrate through the top and bottom electrodes. The PMN-PT substrate was initially in P_r^+ state and the electric field was changed in the sequence of 0 kV/cm$\rightarrow$−7.5 kV/cm$\rightarrow$+7.5 kV/cm$\rightarrow$0 kV/cm. The inset shows the PFM signal (which is in proportional to the induced out-of-plane strain) as a function of bipolar electric potential applied to the PMN-PT substrate.

FIG. 4. (Color online) Temperature dependence of the resistance for the LaMnO$_{3+\delta}$ film at $H=0$, 3, 6, and 9 T when the PMN-PT substrate is in P_r^0 and P_r^+ states, respectively. Inset (a) shows the XRD patterns in the vicinity of (002) reflections for the LaMnO$_{3+\delta}$/PMN-PT structure when the PMN-PT substrate is in P_r^0 and P_r^+ states, respectively. Inset (b) shows ferroelectric-poling-induced relative change in the resistance, $\Delta R/R$, of the LaMnO$_{3+\delta}$ film at $H=0$ T. Here, $\Delta R/R$ is defined as $\Delta R/R=[R(P_r^0,H)-R(P_r^+,H)]/R(P_r^0,H)$. Note that the electric field was turned off after the PMN-PT substrate had been poled to P_r^+ state.

ferroelectric field effect transistor structures. However, if the ferroelectric-poling-induced strain plays a dominant role in influencing the transport properties, the *R-E* hysteresis loop should show a butterflylike shape with the resistance change exhibiting the same sign for opposite directions of applied electric field, as previously observed in La$_{0.7}$Sr$_{0.3}$$MO_3$($M$=Mn,Co)/0.72Pb(Mg$_{1/3}Nb_{2/3}$)O$_3$-0.28PbTiO$_3$ structures.[11,23] We have measured the *R-E* hysteresis loop of the LaMnO$_{3+\delta}$/PMN-PT structure (see Fig. 3). The result shows that the *R-E* hysteresis loop has a butterflylike shape, which is the typical behavior of the resistance change due to the strain induced by the rotation of the polarization direction in the PMN-PT substrate.[11,23] The inset of Fig. 3 shows the electric field induced out-of-plane strain of a PMN-PT single crystal as a function of bipolar electric potential applied to a PMN-PT single crystal, obtained by measurements of the piezoresponse force microscopy (PFM) using a scanning probe microscope operated in the piezoforce mode. Similar to the resistance change shown in Fig. 3, the induced strain shows a butterflylike hysteresis loop, which implies that the butterflylike modulation of the resistance is strain induced. Therefore, we believe that the mechanic distortion of the LaMnO$_{3+\delta}$ film induced by the poling of the substrates plays a dominant role in influencing the transport properties of the LaMnO$_{3+\delta}$ film while the ferroelectric field effect has a minor effect on the electrical properties of the film.

Figure 4 shows the temperature dependence of the resistance for the LaMnO$_{3+\delta}$ film in different magnetic fields H when the PMN-PT substrate is in P_r^0 state and poled state (denoted by P_r^+), respectively. For P_r^0 state and $H=0$ T, the resistance of the film increases with decreasing temperature
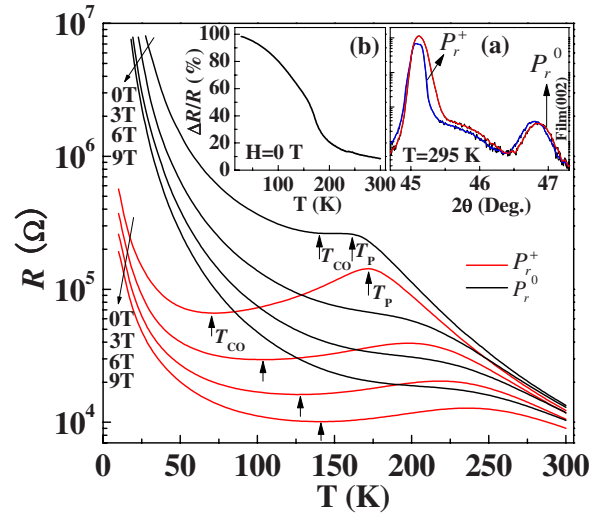
from 300 K and undergoes an insulator-to-metal like transition at $T_P \sim 161$ K. With further decrease in the temperature, the resistance levels off and increases again at $T \sim 141$ K. The overall behavior is quite similar to that observed in the lightly doped (La$_{0.75}$Pr$_{0.25}$)$_{7/8}$Sr$_{1/8}$MnO$_3$,[24] La$_{1-x}$Ca$_x$MnO$_3$ ($x=0.15$ and 0.2),[25] and La$_{1-x}$Sr$_x$MnO$_3$ ($0.11 \le x \le 0.13$) (Ref. 26) bulk materials, for which charge/orbital ordering is observed at low temperatures. We note that charge-ordering transition temperatures (T_{CO}) of $\sim$131, 146, and 152 K for $\delta=0.085$, 0.092, and 0.096, respectively, have been observed in LaMnO$_{3+\delta}$ single crystals by Choi *et al.*[7] Ritter *et al.*[3] also observed the CO phase at temperatures below T_C in LaMnO$_{3+\delta}$ ($\delta=0.07$ and 0.1) polycrystalline samples by measurements of ac initial magnetic susceptibility and neutron diffraction. The upturn of the resistance near $T \sim 141$ K in the present LaMnO$_{3+\delta}$ film is probably due to charge ordering. When the magnetic field is increased, the resistance decreases significantly, thus exhibiting colossal magnetoresistance effect. The insulator-to-metal transition temperature also shifts to a higher temperature.

After the measurements of the resistance as a function of temperature in magnetic fields when the PMN-PT substrate was in P_r^0 state, we applied a dc poling field of +10 kV/cm to the LaMnO$_{3+\delta}$/PMN-PT structure through the top and bottom electrodes so that the PMN-PT substrate was poled to P_r^+ state, as schematically indicated by the arrow in the inset (a) of Fig. 2. It should be pointed out that, after the PMN-PT substrate had been poled to P_r^+ state, the poling field applied to the LaMnO$_{3+\delta}$/PMN-PT structure was turned off. Since the PMN-PT substrate has a ferroelectric Curie temperature of $\sim$155 °C (much higher than room temperature), the po-

larization direction will remain toward the poling direction even if the poling field was turned off. As a consequence, there is a remnant strain in the PMN-PT substrate. *In situ* XRD measurements indicate that, associated with the change in the poling state from P_r^0 to P_r^+ (here, $E=0$ kV/cm), both the PMN-PT(002) and LaMnO$_{3+\delta}$(002) reflections shift to lower 2θ values [see the inset (a) of Fig. 4], implying that the lattice constants c of both the PMN-PT substrate and LaMnO$_{3+\delta}$ film have been elongated as a result of ferroelectric poling. The lattice constant c of the film (c_{film}) is found to increase from 3.875 Å for P_r^0 state to 3.880 Å for P_r^+ state, corresponding to $\Delta c_{film}/c_{film} \sim 0.13\%$. Due to the Poisson effect, the increase in $\Delta c_{film}/c_{film}$ would be accompanied by a decrease in the in-plane tensile strain. As a result, the insulator-to-metal like transition temperature T_P increases from 161 to 172 K, and the resistance at $H=0$ T for P_r^+ state becomes smaller than that for P_r^0 state over the whole temperature range (see Fig. 4). The relative change in the resistance, $\Delta R/R$, defined as $\Delta R/R=[R(P_r^0,H)-R(P_r^+,H)]/R(P_r^0,H)$, is shown in the inset (b) of Fig. 4. It is noted that $\Delta R/R$ increases with decreasing temperature, reaching a high value of 98.2% at 30 K. Moreover, T_{CO} (defined as the temperature where the resistance shows an upturn), decreases from 141 to 70 K when the polarization states change from P_r^0 to P_r^+. This, together with the large decrease in the resistance indicates that the CO phase in the LaMnO$_{3+\delta}$ film is substantially suppressed while the FM metallic phase is stabilized as a consequence of the decrease in the JT distortion due to the reduction in the in-plane tensile strain.

Another important feature of the transport properties is that, whether the PMN-PT substrate is in P_r^0 or P_r^+ state, both T_{CO} and T_P increase significantly with increasing magnetic field, and this effect is particularly noticeable when the PMN-PT substrate is in P_r^+ state. This feature is similar to that observed in lightly doped La$_{7/8}$Sr$_{1/8}$MnO$_3$ single crystals for which both T_{CO} (near 150 K) and T_P (near 196 K) increase with increasing magnetic fields.[27] The similarity in the effects of magnetic field on both T_{CO} and T_P observed in the LaMnO$_{3+\delta}$ film and the charge-ordered La$_{7/8}$Sr$_{1/8}$MnO$_3$ single crystals provides an indirect evidence that the upturn of the resistance near 141 K for P_r^0 state and 71 K for P_r^+ state is associated with a charge-/orbital-ordering phase transition. We note that there are no structural anomalies near $T=141$ and 71 K for the PMN-PT substrate, as revealed by low-temperature XRD measurements.[17]

Figure 5 shows the temperature dependence of the zero-field-cooled (ZFC) and field-cooled (FC) magnetization for the LaMnO$_{3+\delta}$/PMN-PT structure when the PMN-PT substrate is in P_r^0 state. The onset of the ferromagnetic ordering occurs at $T\sim165$ K, which is close to the insulator-to-metal like transition at $T\sim161$ K. With decreasing temperature from 165 K, a pronounced irreversibility is observed at $T_{CG}\sim127$ K between ZFC and FC curves (at $H=50$ G), which is the typical behavior of a magnetic cluster-glass phase, as previously reported for LaMnO$_{3+\delta}$.[28,29] As the field increases the irreversible behavior is reduced and is no longer present at $H=500$ G. The cluster-glass behaviors imply that phase-separation exists (i.e., FM metallic clusters are embedded in an AFM insulating matrix) in the LaMnO$_{3+\delta}$
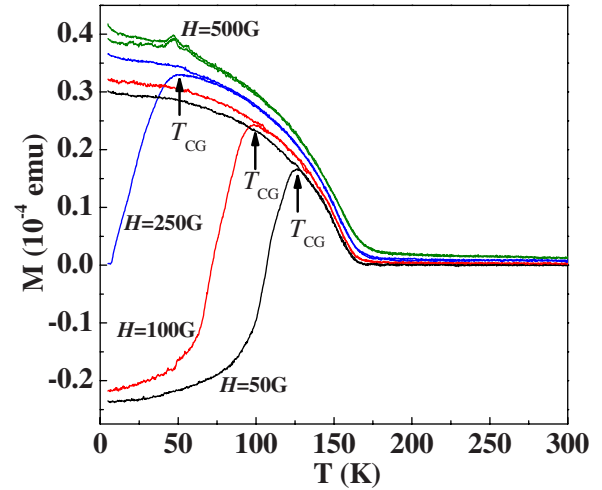

FIG. 5. (Color online) Temperature dependence of the zero-field-cooled (ZFC) and field-cooled (FC) magnetization for the LaMnO$_{3+\delta}$ film when the PMN-PT substrate is in P_r^0 state.

film at low temperatures. Since the excess oxygen ions cannot be accommodated in the interstitial sites of the perovskite structure, the oxidation process is, in fact, accomplished through the formation of equal amounts of La and Mn vacancies.[30] To maintain the charge neutrality, some of Mn^{3+} ions would be oxidized to Mn^{4+} ions. Trapping of Mn^{4+} ions near the cation vacancies introduces local FM metallic clusters within which electron transfer from Mn^{3+} to Mn^{4+} ions introduces FM double-exchange interaction that is stronger than the AFM Mn^{3+}-O-Mn^{3+} superexchange interaction in the host lattice.[31] Because the concentration of Mn vacancies and, hence, of clusters is not high, these FM metallic clusters are separated from one another, giving rise to FM insulating behavior of the resistance at $H=0$ T when the PMN-PT substrate is in P_r^0 state. Nevertheless, associated with the decrease in the electron-lattice coupling due to the reduced in-plane tensile strain in the film, the enhanced hopping of the charge carriers makes it possible for the FM metallic clusters grow in size and merge into larger clusters, causing a large decrease in the resistance at low temperatures and a shift of T_{CO} toward lower temperatures.

The ferroelectric-poling-induced strain also has a remarkable influence on the magnetotransport properties of the LaMnO$_{3+\delta}$ film. In Fig. 6, we present the temperature dependence of the MR at $H=3$, 6, and 9 T for the LaMnO$_{3+\delta}$ film when the PMN-PT substrate is in P_r^0 and P_r^+ states, respectively. Here, MR is defined as MR$=[R(0)-R(H)]/R(0)$, where $R(0)$ and $R(H)$ are the resistance of the film in zero magnetic field and a magnetic field H, respectively. It is interesting that, for any H value, the MR versus T curves for P_r^0 and P_r^+ states have a crossover, indicating that a reduction in the in-plane tensile strain leads to opposite effects on MR, namely, MR is reduced in the low-temperature FM state while MR is enhanced in the high-temperature paramagnetic (PM) state.

To better characterize the effects of the induced strain on MR, we measured MR of the film at various fixed temperatures covering the range from the FM state to PM state. In the inset of Fig. 6, we show the MR versus H curves at 40
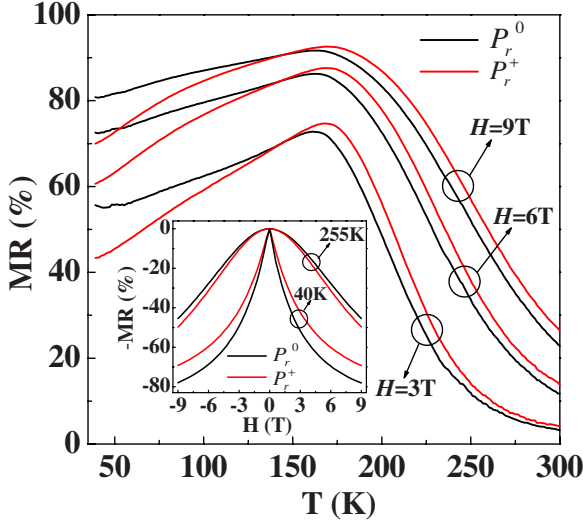
FIG. 6. (Color online) Temperature dependence of MR for the LaMnO$_{3+\delta}$ film at $H=3$, 6, and 9 T when the PMN-PT substrate is in P_r^0 and P_r^+ states, respectively. Inset shows MR versus H curves at $T=40$ and 255 K for the LaMnO$_{3+\delta}$ film when the PMN-PT substrate is in P_r^0 and P_r^+ states, respectively.

FIG. 7. (Color online) Temperature dependence of the resistance-strain coefficient of the LaMnO$_{3+\delta}$ film. The inset shows the relative change in the resistance, $\Delta R/R$, of the LaMnO$_{3+\delta}$ film between the two top-top gold electrodes as a function of the electric field applied to the LaMnO$_{3+\delta}$/PMN-PT structure through the top and bottom electrodes.

and 255 K when the PMN-PT substrate is in P_r^0 and P_r^+ states, respectively. The results clearly indicate that, in comparison with the MR when the PMN-PT substrate is in P_r^0 state, the MR value when the PMN-PT substrate is in P_r^+ state is reduced in the FM state (e.g., 40 K) but enhanced in the PM state, consistent with the behavior of the MR versus T curves shown in Fig. 6. Note that the induced strain has opposite effects on MR in FM and PM states was previously observed for the La$_{0.7}$Ba$_{0.3}$MnO$_3$/PMN-PT structure.[15] The similarity in the behavior of MR between LaMnO$_{3+\delta}$ and La$_{0.7}$Ba$_{0.3}$MnO$_3$ films implies that the underlying mechanism is probably the same. Namely, the effects of the induced strain on MR can be explained in terms of phase separation. In the high-temperature PM insulating state, it is reasonable that a small fraction of FM metallic clusters arising from the local Mn^{3+}-O-Mn^{4+} double exchange are embedded in the PM insulating matrix. Associated with the reduction in the JT distortion induced by the ferroelectric poling, the volume fraction of the FM metallic phase would increase at the expense of the PM insulating phase. As a consequence, MR for P_r^+ state is larger than that for P_r^0 state in the high-temperature PM state.[15]

In the low-temperature FM state, e.g., $T=30$ K, the CO insulating phase coexists with the FM metallic phase with the former dominating over the latter. It is noted that, in the CO state, MR results largely from the magnetic field induced conversion of CO insulating phase to FM metallic phase.[32–34] The large decrease in the resistance (e.g., $\Delta R/R \approx 98.2\%$ at 30 K) induced by ferroelectric poling [inset (b) of Fig. 4] indicates that a considerable fraction of the CO insulating phase have been converted to FM metallic phase due to the decrease in the in-plane tensile strain. That is, the volume fraction of the CO insulating phase in P_r^+ state is smaller than that in P_r^0 state. Therefore, the effective volume fraction of the CO insulating phase that is converted to FM metallic phase in P_r^+ state would be smaller than that in P_r^0 state. So,
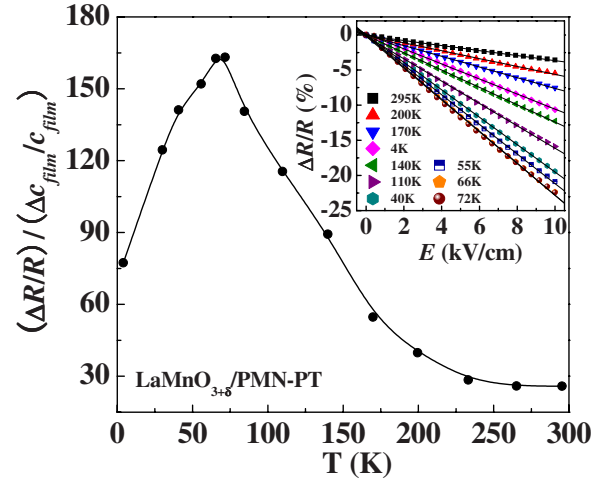
the MR in P_r^+ state is smaller than that in P_r^0 state. We mention here that similar phenomena have been observed in charge-ordered Pr$_{0.5}$Ca$_{0.5}$Mn$_{1-x}$Cr$_x$O$_3$ $(0 \leq x \leq 0.07)$,[32] La$_{0.625-x}$Pr$_x$Ca$_{0.325}$MnO$_3$,[33] and Pr$_{0.5}$Ca$_{0.2}$Sr$_{0.3}$MnO$_{3-\delta}$ (Ref. 34) systems in which the low-temperature MR decreases with increasing volume fraction of FM metallic phase induced by Cr (or La) doping or oxygen deficiencies.

2. Effects of the converse piezoelectric effect on the resistance and strain of the film

After the PMN-PT substrate had been poled to P_r^+ state, we studied the effects of the strain induced by the converse piezoelectric effect on the strain state and transport properties of the LaMnO$_{3+\delta}$ film. The inset of Fig. 7 shows the relative change in the resistance, $\Delta R/R$, of the film between the two top-top gold electrodes as a function of the electric field applied to the LaMnO$_{3+\delta}$/PMN-PT structure through the top and bottom electrodes. One sees that $\Delta R/R$ decreases linearly with increasing electric field at any fixed temperature. Since there are considerable amount of La and Mn vacancies in the film, it is naturally expected that some of these vacancies and/or some lattice-mismatch-induced dislocations would appear at the interface between the film and the substrate, whose state may be affected by the induced strain, thereby influencing the transport properties. Nevertheless, we found that the linear dependence of the resistance on E can be quite well reproduced. We thus believe that the effects of vacancies and/or dislocations on the resistance can be neglected when the strain state of the film is modified by the applied electric field. It is well known that, when an electric field is applied to a poled ferroelectric material, a strain along the direction of the electric field would be induced due to the converse piezoelectric effect.[18] The induced strain ε is proportional to the electric field E, i.e., $\varepsilon = d_{33}E$, where d_{33} is the longitudinal piezoelectric coefficient of the poled
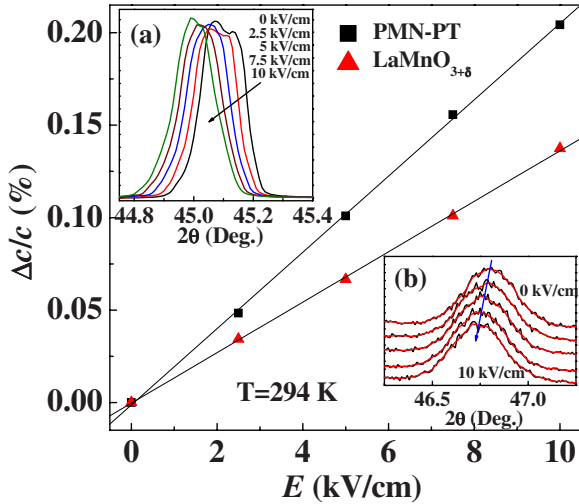
FIG. 8. (Color online) Relative change in the lattice constants c of the PMN-PT substrate and LaMnO$_{3+\delta}$ film as a function of the electric field applied to the LaMnO$_{3+\delta}$/PMN-PT structure. Note that the PMN-PT substrate has already been poled to P_r^+ state before the *in situ* XRD measurements. Insets (a) and (b) show the XRD patterns in the vicinity of (002) reflections for the PMN-PT substrate and LaMnO$_{3+\delta}$ film under different electric fields, respectively.

material.[18] *In situ* XRD measurements on a LaMnO$_{3+\delta}$/PMN-PT structure indicate that both the PMN-PT(002) and LaMnO$_{3+\delta}$(002) reflections systematically shift to lower 2θ values [see the insets (a) and (b) of Fig. 8, respectively] with increasing electric field, indicating that the lattice constants c of both the PMN-PT substrate and the LaMnO$_{3+\delta}$ film have been elongated. As can be seen in Fig. 8, the relative change in the lattice constant c of the PMN-PT substrate, $\Delta c_{PMN-PT}/c_{PMN-PT}$, increases linearly with increasing E, indicating the piezoelectric nature of the induced strain in the substrate.[14] The induced strain was transferred to the film, giving rise to a linear dependence of $\Delta c_{film}/c_{film}$ on E. The relationship between $\Delta R/R$ and $\Delta c_{film}/c_{film}$ can be written as $\Delta R/R = m\Delta c_{film}/c_{film}$, where m is a constant. The resistance-strain coefficient $(\Delta R/R)/(\Delta c_{film}/c_{film})$ of the LaMnO$_{3+\delta}$ film is plotted as a function of temperature in Fig. 7. $(\Delta R/R)/(\Delta c_{film}/c_{film})$ increases with decreasing temperature and reaches a maximal value ($\sim$163) near T_{CO} ($\sim$70 K) and then decreases remarkably with further decreases in the temperature. We note that $(\Delta R/R)/(\Delta c_{film}/c_{film})$ of the LaMnO$_{3+\delta}$ film near T_{CO} is considerably larger than that $[(\Delta R/R)/(\Delta c_{film}/c_{film}) \sim 26-76]$ of La$_{0.7}$Ca$_{0.15}$Sr$_{0.15}$MnO$_3$ thin films grown on PMN-PT substrates.[13] For perovskite manganites exhibiting insulator-to-metal transition, e.g., La$_{0.7}A_{0.3}$MnO$_3$ (A=Ca, Sr), it is generally accepted that there is strong JT electron-lattice coupling in the PM insulating state and the reduction in the JT electron-lattice coupling is mainly responsible for the large decrease in the resistance just below the insulator-to-metal transition temperature.[1,35–37] The observed large resistance-strain coefficient demonstrates that there exists strong JT electron-lattice coupling in the LaMnO$_{3+\delta}$ film.

B. CaMnO$_3$/PMN-PT structure

To obtain more insight into the effects of the JT electron-lattice coupling on the transport properties of LaMnO$_{3+\delta}$
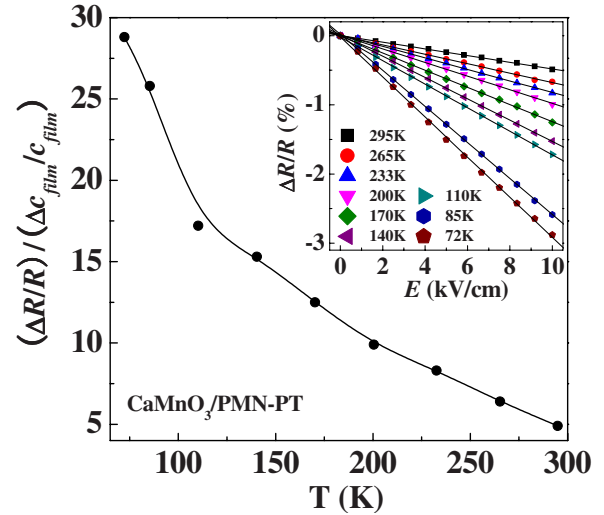

FIG. 9. (Color online) Temperature dependence of the resistance-strain coefficient of the CaMnO$_3$ film. The inset shows the relative change in the resistance, $\Delta R/R$, of the CaMnO$_3$ film between the two top-top gold electrodes as a function of the electric field applied to the CaMnO$_3$/PMN-PT structure through the top and bottom electrodes.

film, we studied the effects of the strain induced by the converse piezoelectric effect on the transport properties of CaMnO$_3$ thin films grown on PMN-PT substrates and compared the results with that of LaMnO$_{3+\delta}$ films. Similar to that observed in the LaMnO$_{3+\delta}$ film, the resistance of the CaMnO$_3$ film at a fixed temperature also decreases linearly with increasing E, as can be seen in the inset of Fig. 9. Although the relative change in the resistance, $\Delta R/R$, is relatively small, the results clearly indicate that a reduction in the in-plane tensile strain leads to a decrease in the resistance of the CaMnO$_3$ film. Based on *in situ* XRD measurements, we found that, when an electric field of 10 kV/cm is applied to the CaMnO$_3$/PMN-PT structure, the relative change in the lattice constant c of the CaMnO$_3$ film, $\Delta c_{film}/c_{film}$, is $\sim$0.1%. The resistance-strain coefficients, $(\Delta R/R)/(\Delta c_{film}/c_{film})$, of the CaMnO$_3$ film at various temperatures are calculated and shown in Fig. 9. It was found that, at the same temperature, $(\Delta R/R)/(\Delta c_{film}/c_{film})$ of the LaMnO$_{3+\delta}$ film is much larger than that of the CaMnO$_3$ film. Since the CaMnO$_3$ film does not show JT distortion, the effects of JT electron-lattice coupling on the transport properties in CaMnO$_3$ film can be neglected. The linearly decrease in the resistance of the CaMnO$_3$ film probably arises from an increase in the electronic bandwidth due to the reduction in the in-plane tensile strain, which leads to a change in the Mn-O bond length and/or the Mn-O-Mn bond angle. It is worth mentioning that the experimental works by Chen *et al.*[38,39] showed that, in lightly doped La$_{0.9}$Sr$_{0.1}$MnO$_3$ thin films, the electron-lattice coupling stemming from the JT distortion is mainly responsible for the effects of substrate-induced strain on the transport and magnetic properties of the film and that the contribution from the electronic bandwidth is much smaller than that from the electron-lattice coupling. We thus believe that the strain-induced modification in the electronic bandwidth alone is not sufficient to account for the

large $(\Delta R/R)/(\Delta c_{film}/c_{film})$ observed in the LaMnO$_{3+\delta}$ film. The effects of the induced strain on the transport properties of the LaMnO$_{3+\delta}$ film is mainly due to the strain-induced weakening of the electron-lattice coupling arising from the reduction in the in-plane tensile strain. This result is in agreement with the theoretical calculation by Ahn and Millis,[40,41] who showed that the strong coupling between electron and lattice is crucial for the understanding of the effects of substrate-induced strain in LaMnO$_3$ thin films.

IV. CONCLUSIONS

In summary, using ferroelectric PMN-PT single crystals as substrates, we have studied the effects of the substrate-induced strain on the strain state and transport properties of LaMnO$_{3+\delta}$ thin films by *in situ* dynamically modifying the lattice strain of the films via ferroelectric poling or the converse piezoelectric effect. Ferroelectric poling (or the converse piezoelectric) induces a significant decrease in the in-plane tensile strain of the film, which reduces the JT electron-lattice coupling, thereby enhancing the volume fraction of the FM metallic phase. As a result, the resistance was reduced; the insulator-to-metal transition temperature T_P was enhanced. Particularly, it was observed that the decrease in the in-plane tensile strain leads to opposite effects on MR above and below T_P, which is found to be closely related to the strain-induced changes in the volume fraction of coexistence phases. Moreover, we have observed that the resistance-strain coefficient $(\Delta R/R)/(\Delta c_{film}/c_{film})$ of LaMnO$_{3+\delta}$ films is much larger than that of CaMnO$_3$ films (for which there is no JT distortion), identifying that the JT distortion plays a very important role in determining the transport properties of LaMnO$_{3+\delta}$ films. The results also show that the strong coupling between electron and lattice is crucial for the understanding of the effects of substrate-induced strain in manganite thin films.

[1] M. B. Salamon and M. Jamie, Rev. Mod. Phys. **73**, 583 (2001).

[2] Y. Murakami, J. P. Hill, D. Gibbs, M. Blume, I. Koyama, M. Tanaka, H. Kawata, T. Arima, Y. Tokura, K. Hirota, and Y. Endoh, Phys. Rev. Lett. **81**, 582 (1998).

[3] C. Ritter, M. R. Ibarra, J. M. De Teresa, P. A. Algarabel, C. Marquina, J. Blasco, J. Garíca, S. Oseroff, and S.-W. Cheong, Phys. Rev. B **56**, 8902 (1997).

[4] F. Prado, R. D. SaHnchez, A. Caneiro, M. T. Causa, and M. Tovar, J. Solid State Chem. **146**, 418 (1999).

[5] J. Töpfer and J. B. Goodenough, J. Solid State Chem. **130**, 117 (1997).

[6] D. Louca, E. L. Brosha, and T. Egami, Phys. Rev. B **61**, 1351 (2000).

[7] K.-Y. Choi, Y. G. Pashkevich, V. P. Gnezdilov, G. Güntherodt, A. V. Yeremenko, D. A. Nabok, V. I. Kamenev, S. N. Barilo, S. V. Shiryaev, A. G. Soldatov, and P. Lemmens, Phys. Rev. B **74**, 064406 (2006).

[8] I. O. Troyanchuk, V. A. Khomchenko, M. Tovar, H. Szymczak, and K. Bärner, Phys. Rev. B **69**, 054432 (2004).

[9] X. O. Bilani-Zeneli, A. D. Rata, A. Herklotz, O. Mieth, L. M. Eng, L. Schultz, M. D. Biegalski, H. M. Christen, and K. Dörr, J. Appl. Phys. **104**, 054108 (2008).

[10] R. B. Gangineni, L. Schultz, C. Thiele, I. Mönch, and K. Dörr, Appl. Phys. Lett. **91**, 122512 (2007).

[11] C. Thiele, K. Dörr, S. Fähler, L. Schultz, D. C. Meyer, A. A. Levin, and P. Paufler, Appl. Phys. Lett. **87**, 262502 (2005).

[12] C. Thiele, K. Dörr, O. Bilani, J. Rödel, and L. Schultz, Phys. Rev. B **75**, 054408 (2007).

[13] R. K. Zheng, Y. Jiang, Y. Wang, H. L. W. Chan, C. L. Choy, and H. S. Luo, Appl. Phys. Lett. **93**, 102904 (2008).

[14] R. K. Zheng, Y. Wang, H. L. W. Chan, C. L. Choy, and H. S. Luo, Appl. Phys. Lett. **92**, 082908 (2008).

[15] R. K. Zheng, Y. Jiang, Y. Wang, H. L. W. Chan, C. L. Choy, and H. S. Luo, Phys. Rev. B **79**, 174420 (2009).

[16] Z. W. Yin, H. S. Luo, P. C. Wang, and G. S. Xu, Ferroelectrics **229**, 207 (1999).

[17] B. Noheda, D. E. Cox, G. Shirane, J. Gao, and Z.-G. Ye, Phys. Rev. B **66**, 054104 (2002).

[18] B. Jaffe, W. R. Cook, Jr., and H. Jaffe, *Piezoelectric Ceramics* (Academic Press, New York, 1971).

[19] N. M. Souza-Neto, A. Y. Ramos, H. C. N. Tolentino, E. Favre-Nicolin, and L. Ranno, Phys. Rev. B **70**, 174451 (2004).

[20] A. J. Millis, T. Darling, and A. Migliori, J. Appl. Phys. **83**, 1588 (1998).

[21] T. Kanki, Y.-G. Park, H. Tanaka, and T. Kawai, Appl. Phys. Lett. **83**, 4860 (2003).

[22] T. Zhao, S. B. Ogale, S. R. Shinde, R. Ramesh, R. Droopad, J. Yu, K. Eisenbeiser, and J. Misewich, Appl. Phys. Lett. **84**, 750 (2004).

[23] A. D. Rata, A. Herklotz, K. Nenkov, L. Schultz, and K. Dörr, Phys. Rev. Lett. **100**, 076401 (2008).

[24] J. Geck, P. Wochner, S. Kiele, R. Klingeler, A. Revcolevschi, M. v. Zimmermann, B. Büchner, and P. Reutler, New J. Phys. **6**, 152 (2004).

[25] G.-L. Liu, J.-S. Zhou, and J. B. Goodenough, Phys. Rev. B **70**, 224421 (2004).

[26] B. Dabrowski, X. Xiong, Z. Bukowski, R. Dybzinski, P. W. Klamut, J. E. Siewenie, O. Chmaissem, J. Shaffer, C. W. Kimball, J. D. Jorgensen, and S. Short, Phys. Rev. B **60**, 7006 (1999).

[27] S. Uhlenbruck, R. Teipen, R. Klingeler, B. Büchner, O. Friedt, M. Hücker, H. Kierspel, T. Niemöller, L. Pinsard, A. Revcolevschi, and R. Gross, Phys. Rev. Lett. **82**, 185 (1999).

[28] S. N. Barilo, V. I. Gatal'skaya, S. V. Shiryaev, G. L. Bychkov, L. A. Kurochkin, S. N. Ustinovich, R. Szymczak, M. Baran, and B.

Krzymańska, Phys. Solid State **45**, 146 (2003).

[29] L. Ghivelder, I. A. Castillo, M. A. Gusmão, J. A. Alonso, and L. F. Cohen, Phys. Rev. B **60**, 12184 (1999).

[30] J. A. M. van Roosmalen and E. H. P. Cordfunke, J. Solid State Chem. **110**, 109 (1994).

[31] J. Töpfer and J. B. Goodenough, Chem. Mater. **9**, 1467 (1997).

[32] S. X. Cao, W. J. Li, J. C. Zhang, B. J. Kang, T. Gao, and C. Jing, J. Appl. Phys. **102**, 053909 (2007).

[33] M. Uehara, S. Mori, C. H. Chen, and S.-W. Cheong, Nature (London) **399**, 560 (1999).

[34] D. Niebieskikwiat, A. Caneiro, and R. D. Sánchez, J. Appl. Phys. **93**, 8080 (2003).

[35] A. J. Millis, P. B. Littlewood, and B. Shraiman, Phys. Rev. Lett. **74**, 5144 (1995).

[36] A. J. Millis, Nature (London) **392**, 147 (1998).

[37] C. H. Booth, F. Bridges, G. H. Kwei, J. M. Lawrence, A. L. Cornelius, and J. J. Neumeier, Phys. Rev. Lett. **80**, 853 (1998).

[38] X. J. Chen, S. Soltan, H. Zhang, and H.-U. Habermeier, Phys. Rev. B **65**, 174402 (2002).

[39] X. J. Chen, H.-U. Habermeier, H. Zhang, G. Gu, M. Varela, J. Santamaria, and C. C. Almasan, Phys. Rev. B **72**, 104403 (2005).

[40] K. H. Ahn and A. J. Millis, Physica B **312-313**, 766 (2002).

[41] K. H. Ahn and A. J. Millis, Phys. Rev. B **64**, 115103 (2001).